Eur. Phys. J. D **35**, 307–312 (2005)
DOI: 10.1140/epjd/e2005-00087-7

The European Physical Journal D

Measurements of thermal electron attachment rate coefficients to molecules using an electron swarm technique

C.A. Mayhew[1,a], A.D.J. Critchley[1], D.C. Howse[2], V. Mikhailov[1], and M.A. Parkes[1]

[1] School of Physics and Astronomy, University of Birmingham, Edgbaston B15 2TT, UK
[2] Walsall College of Arts and Technology, St. Pauls Street, Walsall WS1 1XN, UK

Received 7 March 2005
Published online 14 June 2005 –

Abstract. An existing electron swarm apparatus has been redesigned and upgraded. In particular, the new design incorporates a novel planar radioactive foil to form an integral part of the drift tube, allowing us to overcome inherent problems present in our earlier system which used a cylindrical radioactive source. In addition to this, substantial upgrades have been made to improve the gating and amplification electronics and the data acquisition system. This has resulted in a much greater signal to noise ratio and improved accuracy. This paper describes the upgraded apparatus and its use in obtaining thermal (300 K) attachment rate coefficients to a number of molecules. The quality of the measurements and data are illustrated through the measurement of the thermal attachment rate coefficient for SF_6 ($k_{th}(SF_6) = (2.38 \pm 0.15) \times 10^{-7}$ cm^3 s^{-1}). Thermal electron attachment rate coefficients for four other molecules are presented, namely for two derivatives of SF_6, SF_5CF_3 and SF_5Cl, and two perfluorocarbons, c-C_4F_8 and 2-C_4F_8.

PACS. 34.80.Lx Electron-ion recombination and electron attachment – 34.80.Ht Dissociation and dissociative attachment by electron impact – 82.20.Pm Rate constants, reaction cross sections, and activation energies

1 Introduction

The study of electron capture processes is an active area of research. By its very nature it is multidisciplinary, fundamental, and of practical value. Electron attachment data need to be incorporated into models used to characterize gaseous discharges and industrial plasmas. The creation of reactive intermediate species, via dissociative electron attachment, initiate and drive chemical and physical changes in many diverse environments ranging from interstellar molecular clouds to technological plasmas, through to living tissue [1–7].

Many electron attaching gases show a maximum in their electron attachment cross-section at zero electron energy, with values which are comparable with the theoretical upper limit for thermal electron capture. A recent review by Hotop et al. has highlighted the interest in low-energy electron collisions with molecules (and clusters) [8]. As explained in Hotop's review, the experimental techniques which provide high resolution data of resonance and threshold phenomena provide only relative cross-sections. To place these on absolute scales requires knowledge of the thermal energy electron attachment rate coefficients. Accurate determinations of these rate coefficients are therefore needed for many molecules. A further motivation for such measurements comes from the importance of the thermal electron attachment mechanism in many chemical environments, and the study of such processes provides information critical to the understanding of how these environments evolve.

The majority of thermal electron attachment rate coefficients have been obtained using a flowing afterglow Langmuir probe (FALP) technique [9]. Swarm studies have also been used to obtain thermal rate coefficients. The majority of these are based on data derived from measurements with a non-zero value of the reduced electric field strength (see later). Whilst the departure from thermal equilibrium may be small, the experiments do not provide a direct measurement. A simple change in the buffer gas, from the commonly used nitrogen, argon or helium to carbon dioxide results in the electron swarm having a thermal electron energy distribution over a large range of reduced electric field strength values. The use of CO_2 as a buffer gas has been used to investigate thermal electron attachment to great effect by Szamrej et al. [10,11].

In this present work, we describe thermal electron attachment using a swarm apparatus for a number of molecules. For this project, we took the opportunity to redesign and upgrade our drift tube, electronics and data acquisition to remove some inherent problems resulting from using an ion mobility spectrometer for such studies. These adaptations are described in this article.

[a] e-mail: c.mayhew@bham.ac.uk

2 Experimental details

The fundamental importance of electron attachment processes, together with desirable practical applications of these processes, has led to many measurements of electron attachment cross-sections and rate constants of molecules. Several experimental methods have been developed for such measurements, including the flowing afterglow-Langmuir probe [9], threshold photoionisation [8], electron beam (coupled with molecular beam [12] or gas collision chamber [13]) and the electron swarm techniques [14–16]. As mentioned above, for thermal electron energy distributions the flowing afterglow technique has been successfully used to obtain capture rate constants. In addition it is used to identify anion products, something that is not commonly available using electron swarm apparatus. For electron energies above the thermal value, the electron beam and electron swarm techniques have been extensively used.

Beam studies investigate electron attachment processes using nearly mono-energetic electrons over an energy range of typically 0.1–15 eV. The capture occurs under collision free conditions. Relative attachment cross-sections and competing decay channels as a function of electron energy are obtained. The technique is used to identify stable, long-lived anions ($\tau > 10^{-6}$ s). The transmission of anions in beam experiments not only depends on mass filter discrimination, but as Cicman et al. have shown the ion extraction efficiency in crossed beam experiments using trochoidal electron monochromators is also dependent on the kinetic energy release of the anion products produced by dissociative electron attachment [17]. Fragment anions with higher kinetic energies are found to have reduced extraction efficiencies. Almost zero extraction potentials are required to produce ion extraction efficiencies which are independent of the kinetic energy release so that reliable relative cross-sections can be obtained.

Swarm measurements provide absolute data averaged over a broad (and usually non-thermal) electron energy distribution. The attachment takes place in a high pressure environment (typically 1 atmosphere or greater) so that collisional relaxation of the excess internal energy in the anions produced from electron attachment may take place.

The electron swarm technique has resulted in a large body of data on electron attachment processes, most notably from the work by Christophorou and colleagues. The technique relies on the production of pulses of electrons, thereby ensuring that they are temporally distinct from the anion products, in a drift chamber containing a non-electron attaching buffer gas of number density N. Under the influence of an applied electric field E, the electrons are drawn through the gas towards a collector plate, where the intensity of the electron pulses can be measured. Within the drift region, electrons usually attain a non-thermal equilibrium energy distribution, $f(\varepsilon)$, determined by a dynamic balance between the kinetic energy gained from the electric field and energy loss through multiple collisions with the molecules of the buffer gas. Thus $f(\varepsilon)$ primarily depends on the nature of the buffer gas and the ratio E/N. This distribution has been well characterized for a number of gases, e.g. He, Ar and N_2. Trace amounts of an electron attaching gas mixed into the buffer gas results in the removal of electrons, without changing the electron energy distribution. The electron pulse intensity is subsequently reduced at the detector. This reduction in intensity is used in swarm experiments to obtain absolute values of the density reduced electron attachment rate coefficient, from which, with knowledge of the mean electron drift velocities, the electron attachment rate coefficient as a function of mean electron energy can be determined. Electron attachment cross-sections, $\sigma(\varepsilon)$, as a function of electron energy, ε, can in principle be determined by deconvoluting the swarm data, because $f(\varepsilon)$ is known as a function of E/N.

We have developed the electron swarm technique by attaching a mass spectrometer to a drift tube used for swarm studies. A 70 μm orifice in the collector permits product anions to pass into a region of the instrument where they are focussed and mass analysed. This instrument, called an Electron Swarm Mass Spectrometer (ESMS) therefore has the capability of identifying anion products resulting from electron attachment inside the drift tube [18]. This provides valuable additional information on electron capture processes, allowing the mechanisms involved to be elucidated. A similar instrument has been developed by the group of Grimsrud et al., which has been used most notably to investigate electron attachment to $POCl_3$ and $PSCl_3$ [19,20].

The ESMS we have used for our studies of electron attachment processes has been described in detail in the literature [18]. Recently, we have modified the drift chamber of our instrument for the following reasons. In our original design, electrons are produced via ionization of the buffer gas by electrons emitted from a cylindrical 11 mCi ^{63}Ni β-ray source. To minimize electron attachment between the source and drift tube, two buffer gas flows are required; one through the ionization source and the other (in the opposite direction) through the drift tube. This has the potential of leading to flows of gases of different chemical composition, which in turn leads to concentration gradients. These are difficult to predict and/or control. Furthermore, the electric field close to the source region is not uniform, leading to uncertainties in the electron energy distribution around this region. The new design of drift tube uses a planar ^{63}Ni radioactive source, which forms an integral part of the drift tube. This allows the use of a single gas stream to fill all parts of the chamber, eliminating any inhomogeneity in gas concentration and uncertainties in the reaction length. Varying electric field gradients between the electron source and electrical gate are also eliminated. Figure 1 presents a schematic diagram of the new drift tube.

As in our initial design [18], metal ring electrodes inside a glass envelope form the drift tube. The rings are made of aluminium, and are coated with molybdenum to reduce charging effects. They are physically separated from each other by 1 mm ceramic spacers, but are electrically

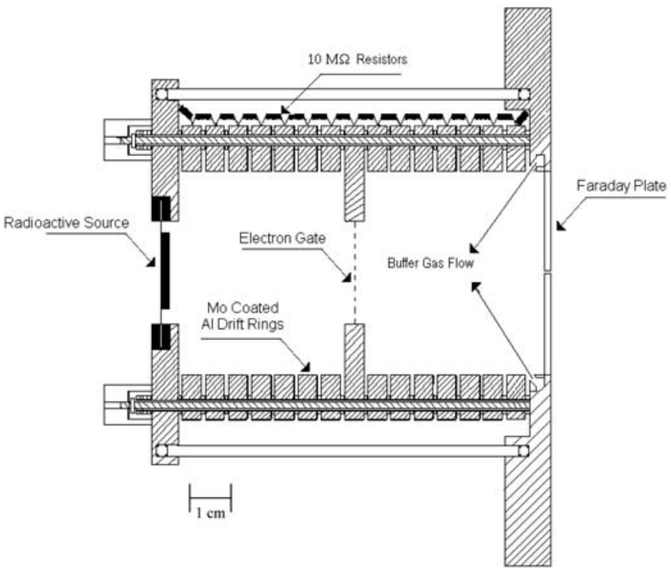

Fig. 1. A schematic representation of the new drift tube used in our electron swarm investigations. The diagram represents a cross-section of the cylindrically symmetric drift tube.

connected via a chain of 10 MΩ resistors. The drift tube is 9.7 cm long, measured from the radioactive source to the Faraday plate. The Faraday plate is electrically isolated from the drift tube, but is normally held at ground potential.

The electron gate is used to convert the constant stream of electrons produced in the source region into a chain of pulses. The gate is based on the Bradbury-Nielsen design, consisting of two interdigitated wire arrays [21]. A dual tracking regulator is used to produce up to ±30 V, on the wire arrays. For optimum performance we have found that one array should be held at a potential of 22 V above the voltage of the drift tube at the position of the gate, V_d, and the other at 22 V below V_d. When the gate is closed, electrons experience a large electric field deflecting them sideways, stopping them from entering the remaining section of the drift tube. To open the gate, the potentials on the arrays are simultaneously switched to V_d for typically 1 ms at a frequency of 25 Hz.

Originally, the gate pulse switching circuit (consisting of an opto-isolator and two Schmitt triggers) was powered by a number of rechargeable batteries. This caused problems as the batteries became discharged, because the gate was not closing properly. Improvements have been made by deriving the power from the mains electricity supply (using a 5 kV flash tested isolation transformer). De-coupling of a 50 Hz signal picked up from the supplies and detected on the Faraday Plate was filtered out by a high voltage low frequency filter.

The Faraday plate collects the electrons and anions that pass through the drift tube. The electron current pulse is converted to a voltage pulse by a current to voltage converter. The signal is amplified by a fast preamplifier, which is housed in a radio frequency shielded case. Switched gain ranges of 10^{-9} A/V to 10^{-6} A/V allow the measurement of electron swarm currents over the range of 1 nA to 1 μA. The amplified pulse is passed to a National Instruments data acquisition card (PCI-6014), where it is digitised. The data are acquired using a customised LabVIEW application. A measurement is obtained by averaging over several hundred pulses and integrating over the whole pulse width. This integration over the whole pulse width has dramatically improved our signal-to-noise ratio.

The determination of the density normalized electron attachment coefficient, α, is readily deduced in the following straightforward manner. Let the intensity of electrons at $x = 0$, the start of the drift tube, be I_0. Between the source and the gate, separated by a distance l_1, diffusion and attachment of electrons occur, so that the electron intensity at the gate will be $I(l_1)$ such that

$$I\left(l_1\right) = I_0 e^{-(n\alpha+\beta)l_1} \tag{1}$$

where β is the diffusive loss coefficient (defined as the probability of diffusive loss of electrons per unit length) and n is the number density of the electron attaching molecule, which is entrained in the buffer gas flow. A fraction of $I(l_1)$, γ, is pulsed into the next section of the drift tube. The initial intensity of the pulse in this section is $A(l_1)$, where

$$A\left(l_1\right) = \gamma I\left(l_1\right) = \gamma I_0 e^{-(n\alpha+\beta)l_1}. \tag{2}$$

As this electron pulse propagates down the drift tube further diffusional and attachment loss of electrons will occur, so that the amplitude of the pulse at the Faraday plate will be $A(l_2)$, where

$$A\left(l_2\right) = A\left(l_1\right) e^{-(n\alpha+\beta)(l_2-l_1)} = \gamma I_0 e^{-\beta l_2} e^{-n\alpha l_2} \tag{3}$$

with l_2 representing the total length of the drift tube. α can then be readily determined from

$$\alpha = -\ln\left\{A\left(l_2\right)/\gamma I_0 e^{-\beta l_2}\right\}/nl_2 \tag{4}$$

which is independent of the position of the gate in the drift tube. A measurement of $\ln A(l_2)$ as a function of n for a fixed E/N is made. Typically 5–8 concentrations (including $n = 0$) are used. The maximum concentration is chosen to produce an attenuation of the pulse amplitude of about 90%. A typical data set is illustrated in Figure 2. A linear least-squares fit of such data, with all points weighted equally gives $\alpha(E/N)$. By multiplying the density normalized electron attachment coefficients by the appropriate mean electron drift velocities, the electron attachment rate constants, $k_a(E/N)$, are obtained.

Most swarm studies have been performed in buffer gases within which the electron energy distribution is dependent on E/N. However, as mentioned earlier, by using CO_2 as the buffer gas an electron swarm with a thermal energy distribution over a large range of E/N values can be created. A determination of the thermal attachment rate coefficient, k_{th}, is then directly possible from the absolute measurement of α through the equation:

$$k_{th} = \mu \frac{E}{N} \alpha \tag{5}$$

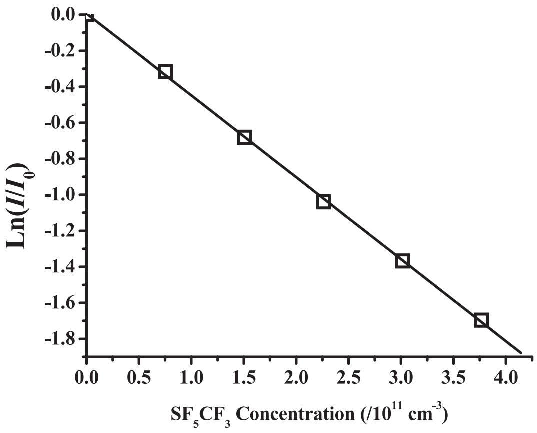

Fig. 2. Plot of a typical data set for determining the density normalised electron attachment coefficient (in this case for the molecule SF_5CF_3). The figure shows the natural logarithm of the normalised electron current pulses (I/I_0), where I_0 is the initial electron current pulse (i.e. at $[SF_5CF_3] = 0$), versus SF_5CF_3 number density taken at $E/N = 8.87 \times 10^{-18}$ V cm^2. For this particular data set, the gradient of linear fit is -4.5×10^{-12} cm^3, from which we can determine that $\alpha = 4.63\times10^{-13}$ cm^2.

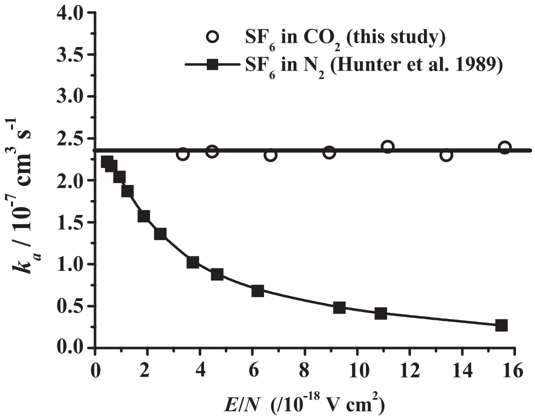

Fig. 3. The dependence of the electron attachment rate constants on E/N for SF_6 determined in a swarm environment using N_2 (from the work of Hunter et al. [23]) and CO_2 buffer gases.

where μ is the electron mobility, which in turn is determined from

$$\mu = \mu_N \left(\frac{1013}{P}\right)\left(\frac{T}{273}\right) \quad (6)$$

where μ_N is the reduced electron mobility, and P and T are the atmospheric pressure (in mbar) and temperature (in Kelvin), respectively, at which the measurements are taken. From measuring the times taken for electron pulses to travel from the gate to the Faraday plate for given E/N values, we have determined a value for μ_N to be $(1.81 \pm 0.05) \times 10^{22}$ V^{-1} cm^{-1} s^{-1}. This value is in good agreement with other values to be found in the literature [22,23].

As mentioned earlier a unique aspect of our apparatus, is its ability to record mass spectra of the anion products resulting from electron attachment in a high pressure environment. In this upgrade, we now use LabVIEW to not only control the mass spectrometer, but also to record mass spectra. Mass spectra are recorded as a function of the electron attaching gas concentration to allow for any anion-molecule reactions in the drift tube. Voltages between the Faraday plate and a sample cone, leading to the mass spectrometer, are kept to sufficiently low values to minimise collision induced dissociation, whilst at the same time high enough to obtain a reasonable anion signal.

3 Results

3.1 Thermal electron attachment rate measurements of SF_6

SF_6 is the best known electronegative gas. Despite concerns associated with its greenhouse properties, SF_6 appears to be the most suitable molecule for many industrial applications in which its electron capture properties for low energy electrons is crucial. This includes its uses as an insulating medium in high-voltage transmission and distribution and in plasma etching.

Owing to its importance, many measurements of the thermal value of the total electron attachment rate coefficient of SF_6 have been made, and whilst there is some variation in the values, the currently recommended value averaged from a number of reliable data, is 2.25×10^{-7} cm^3 s^{-1} [24]. Given the quality of earlier thermal measurements, SF_6 is an ideal molecule for us to test the new drift tube incorporating the planar radioactive source, and operating in a CO_2 buffer gas. We obtained values of k_{th} over a range of E/N ($\sim$0–16 $\times$ 10^{-18} V cm^2). In addition, for each E/N we prepared up to five SF_6 samples diluted in CO_2 prior to injection into the drift tube, in order to check the error associated with determining the concentration of SF_6. Figure 3 shows k_{th}(300 K) measured for SF_6 over the range of E/N used. For comparison, the rate coefficients measured by Hunter et al. [16] in an N_2 buffer gas over the same E/N range are shown. The constancy of the electron attachment rate constant for SF_6 measured using a CO_2 buffer gas throughout the E/N range shown in Figure 2 serves to illustrate that the electron energy distribution in the swarm environment is thermal. Any deviation from the thermal energy distribution as E/N increased would have resulted in a decrease in the measured value of k_{th}. Szamrej and Forys have also shown the constancy of k_{th} for a range of E/N values in their study of multi-body electron attachment processes using CO_2 as a buffer gas [25]. That the electron energy distribution corresponds to that of a thermal one is confirmed further from the value we obtained for $k_{th}(SF_6)$. The swarm data provides a thermal (300 K) electron attachment rate coefficient for SF_6 of $k_{th}(SF_6) = (2.38 \pm 0.15) \times 10^{-7}$ cm^3 s^{-1}, which agrees extremely well with the value determined by Hunter et al. through extrapolation [16], $(2.3 \pm 0.1) \times 10^{-7}$ cm^3 s^{-1} and with the currently recommended value of 2.25×10^{-7} cm^3 s^{-1}. Such agreements provide confidence in the technique described above.

3.2 Thermal electron attachment rate coefficients of SF_5CF_3, SF_5Cl, c-C_4F_8 and 2-C_4F_8

Following the successful SF_6 measurements, we have measured the thermal electron attachment rate coefficients for a number of molecules. This includes two derivatives of SF_6, namely SF_5CF_3 and SF_5Cl, and two perflurorcarbons; c-C_4F_8 and 2-C_4F_8.

The results for the two derivatives of SF_6 are as follow; $k_{th}(SF_5CF_3) = (8.0 \pm 0.3) \times 10^{-8}$ cm^3 s^{-1}, $k_{th}(SF_5Cl) = (2.0 \pm 0.3) \times 10^{-8}$ cm^3 s^{-1}, both measured at room temperature (300 K). Both of these values are below the expected s-wave capture value. The value we have obtained for SF_5CF_3 agrees well with a FALP determination by Miller et al., who obtained $k_{th}(SF_5CF_3) = (8.6 \pm 2.2) \times 10^{-8}$ cm^3 s^{-1} [26]. To our knowledge no other value of $k_{th}(SF_5Cl)$ appears in the literature.

Perfluorocyclobutane (c-C_4F_8) is gas commonly used in semiconductor processing applications. c-C_4F_8 has the potential to be used as a gaseous dielectric, particularly within c-C_4F_8/SF_6 mixtures, which are easier to recover from liquefaction than other combinations. This, together with its electron attachment properties, leads to its potential use as an additive to SF_6 used as a gaseous dielectric [27]. Interest in this molecule also stems from its global warming potential. Based on atmospheric removal by electron attachment, Morris et al. have estimated that its atmospheric lifetime is 1400 years, leading to a high global warming potential [28].

There have been a significant number of measurements of the thermal electron attachment rate coefficient, with values ranging from $(0.4 \pm 0.1) \times 10^{-9}$ cm^3 s^{-1} using an ion cyclotron resonance (ICR) technique [29] to 2.1×10^{-9} cm^3 s^{-1} obtained from a swarm technique [30]. Ignoring any ICR results, Christophorou and Olthoff have given $k_{th}(c\text{-}C_4F_8) = 1.5 \times 10^{-8}$ cm^3 s^{-1}, obtained from an average of eight room-temperature measurements [24]. The value we have obtained $k_{th}(c\text{-}C_4F_8) = (1.81 \pm 0.17) \times 10^{-8}$ cm^3 s^{-1} is in good agreement with this average value, and is in even better agreement with the value of 1.81×10^{-8} cm^3 s^{-1} obtained by Christodoulides et al. [31].

There have been fewer measurements of the thermal electron attachment rate coefficient of 2-C_4F_8. We have obtained a value of $(4.2 \pm 0.2) \times 10^{-8}$ cm^3 s^{-1} in good agreement with a value of 4.8×10^{-8} cm^3 s^{-1} obtained by Christophorou [32].

3.3 Anion products resulting from electron attachment

Mass spectra for low electron attachment to c-C_4F_8 and 2-C_4F_8 have been reported by Christophorou et al. [32]. Low energy electron attachment to c-C_4F_8 results only in the parent anion via non-dissociative electron attachment, i.e. $e^- + c\text{-}C_4F_8 \rightarrow c\text{-}C_4F_8^-$, which is the only product we have observed for our thermal measurements. For 2-C_4F_8, Christophorou et al. observed that by far the main product anion is the parent. However in addition, and with very small branching ratios, $C_4F_7^-$ and $C_4F_6^-$ anions were observed [32]. In our swarm apparatus, we only observed the parent anion. This suggests that the time scale for collisional stabilisation of the parent anion in our swarm experiment must be shorter than the lifetime for dissociation of the parent anion to the above anion products.

Unlike the two perfluorocarbons, the two derivatives of SF_6 attach electrons predominantly via dissociative processes, and only for SF_5Cl is the parent anion observed:

$$e^- + SF_5CF_3 \rightarrow (SF_5CF_3^-)^* \rightarrow SF_5^- + CF_3\,(100\%)$$
$$e^- + SF_5Cl \rightarrow (SF_5Cl^-)^* \rightarrow SF_5^- + Cl\,(90\%)$$
$$\hookrightarrow SF_5Cl^-\,(10\%)$$

these branching ratios are in good agreement with our non-thermal electron swarm measurements [33,34].

4 Conclusions

We have incorporated a planar radioactive source into the drift tube of an electron swarm apparatus. This provides a much more uniform electric field down the axis of the tube. We have improved the gating and amplification electronics and the data acquisition. This redesign and upgrade has led to considerable improvements in signal-to-noise ratio and accuracy of data obtained using our electron swarm apparatus.

We wish to thank the EPSRC for funding this project (GR/S21557/01).

References

1. *Database Needs for Modelling and Simulation of Plasma Processing* (National Research Council, National Academy Press, Washington DC, 1996)
2. *Electron-Driven Processes: Scientific Challenges and Technological Opportunities* (National Research Council, National Academy Press, Washington DC, 2000)
3. B. Boudaïffa, P. Cloutier, D. Hunting, M.A. Huels, L. Sanche, Science **287**, 1658 (2000)
4. M.A. Huels, L. Sanche, I. Hahndorf, E. Illenberger, J. Chem. Phys. **108**, 1309 (1998)
5. H. Abdoul-Carime, M.A. Huels, L. Sanche, F. Brüning, E. Illenberger, J. Chem. Phys. **113**, 2517 (2000)
6. H. Abdoul-Carime, M.A. Huels, L. Sanche, E. Illenberger, J. Am. Chem. Soc. **123**, 5354 (2001)
7. G. Hanel, B. Gstir, S. Denifl, P. Scheier, M. Probst, B. Farizon, E. Illenberger, T.D. Märk, Phys. Rev. Lett. **90**, 188104-1 (2003)
8. H. Hotop, M.W. Ruf, M. Allan, I.I. Fabrikant, Adv. At. Mol. Opt. Phys. **49**, 85 (2003)
9. D. Smith, P. Ŝpanel, Adv. At. Mol. Opt. Phys. **32**, 307 (1994)
10. W. Barszczewska, J. Kopyra, J. Wnorowska, I. Szamrej, J. Phys. Chem. **107**, 11427 (2003)

11. W. Barszczewska, J. Kopyra, J. Wnorowska, I. Szamrej, Int. J. Mass Spectrom. Ion Proc. **233**, 199 (2003)
12. M. Fenzlaff, R. Gerhard, E. Illenberger, J. Chem. Phys. **88**, 149 (1988)
13. L.E. Kline, D.K. Davies, C.L. Chen, P.J. Chantry, J. Appl. Phys. **50**, 6789 (1979)
14. L.G. Christophorou, E.L. Chaney, A.A. Christodoulides, Chem. Phys. Lett. **3**, 363 (1969)
15. L.G. Christophorou, D.L. McCorkle, A.A. Christodoulides, *Electron-Molecule Interactions and Their Applications* (Academic Press, New York, 1984)
16. S.R. Hunter, J.G. Carter, L.G. Christophorou, J. Chem. Phys. **90**, 4879 (1989)
17. P. Cicman, M. Francis, J.D. Skalny, T.D. Märk, Int. J. Mass Spectrom. **223/224**, 271 (2003)
18. G.K. Jarvis, R.A. Kennedy, C.A. Mayhew, Int. J. Mass Spectrom. Ion Proc. **205**, 253 (2001)
19. D.H. Williamson, C.A Mayhew, W.B Knighton, E.P. Grimsrud, J. Chem. Phys. **113**, 11036 (2000)
20. W.B. Knighton, T.M. Miller, E.P. Grimsrud, A.A. Viggiano, J. Chem. Phys. **120**, 211 (2004)
21. L.G. Huxley, R.W. Crompton, *The Diffusion and Drift of Electrons in Gases*, Wiley Series in Plasma Physics (Wiley-Interscience, New York, 1974), Chap. 10, pp. 297-370
22. O.W. Dmitriev, W. Tchórzewska, I. Szamrej, M. Foryś, Radiat. Phys. Chem. **40**, 547 (1992)
23. E.B. Wagner, F.J. Davis, G.S. Hurst, J. Chem. Phys. **47**, 3138 (1967)
24. L.G. Christophorou, J.K. Olthoff, *Fundamental Electron Interactions with Plasma Processing Gases* (Kluwer Academic/Plenum Publishers, New York, 2004)
25. I. Szamrej, M. Forys, Radiat. Phys. Chem. **33**, 393 (1989)
26. T.M. Miller, S.T. Arnold, A.A. Viggiano, W.B. Knighton, J. Chem. Phys. **116**, 6021 (2002)
27. S. Hamada, T. Takuma, O. Yamamoto, in *Gaseous Dielectrics IX*, edited by L.G. Christophorou, J.K. Olthoff (Kluwer Academic/Plenum Press, New York, 2001), pp. 301-306
28. R.A. Morris, T.M. Miller, A.A. Viggiano, J.F. Paulson, S. Solomon, G. Reid, J. Geophys. Res. **100**, 1287 (1995)
29. R.L. Woodin, M.S. Foster, J.L. Beauchamp, J. Chem. Phys. **72**, 4423 (1980)
30. L.G. Christophorou, D.L. McCorkle, D. Pittman, J. Chem. Phys. **60**, 1182 (1974)
31. A.A. Christodoulides, L.G. Christophorou, D.L. McCorkle, Chem. Phys. Lett. **139**, 350 (1987)
32. I. Sauers, L.G. Christophorou, J.G. Carter, J. Chem. Phys. **71**, 3016 (1979)
33. R.A. Kennedy, C.A. Mayhew, Int. J. Mass Spectrom. Ion Processes **206**, vii (2001)
34. C.A. Mayhew, G.K. Jarvis, A. Critchley, Int. J. Mass Spectrom. **233**, 259 (2004)